Generation of Equivalent Circuit from Finite Element Model Using Model Order Reduction

Yuki Sato[1,2], and Hajime Igarashi[1], *Member, IEEE*

[1]Graduate School of Science and Technology, Hokkaido University, Sapporo, 060-0814, Japan
[2]Research Fellow of the Japan Society for the Promotion of Science (JSPS), Tokyo, 102-0083, Japan

This paper proposes equivalent-circuit generation from the finite element (FE) model of electromagnetic devices using model order reduction (MOR). In this method, an equivalent circuit is directly generated from the reduced transfer function obtained using MOR based on Padé approximation via the Lanczos process. It is shown that the generated circuit yields sufficiently accurate results in both frequency and time domains. Moreover, the computational time of the present method is much shorter than that of circuit generation based on frequency sweep using the conventional FE analysis.

***Index Terms*—DC-DC converter, equivalent circuit, finite element method, model order reduction.**

I. Introduction

Finite Element method (FEM) has been widely used to design electric machines and electromagnetic devices. On the other hand, because of heavy computational burden in FE analysis, they are often modeled as an equivalent circuit for design of their control and driving circuits. The frequency-invariant resistance and reactance in the equivalent circuits can be obtained by FE analysis. However, these equivalent circuit models become inaccurate if the circuit parameters are dependent on frequency due to skin and proximity effects. The circuit parameters can also be determined directly from the frequency response obtained by FE analysis [1]. The computational time required for this method would be, however, too expensive for real uses.

Recently it has been pointed out that the equivalent circuit can directly be generated from the exact solutions to eddy current problems [2]. Although this method is promising from aspects of numerical accuracy and computational complexity, it can only treat simple structures such as plates and cylinders.

In this paper, we propose a new method to generate equivalent method directly from reduced FE models constructed by the model order reduction (MOR) technique [3]-[8]. In this method, the equivalent circuit is generated from the reduced transfer function of an electromagnetic device obtained by Padé approximation via the Lanczos process (PVL) [3][4]. This method can be applied to complicated objects and it provides highly accurate results over all frequency range with small computational burden. It is also possible to employ MOR based on the proper orthogonal decomposition [5]-[8] for this purpose, which is discussed in another contribution [8]. To test the performance of the proposed method, we apply it to inductor models in which the skin and proximity effects are not negligible.

Manuscript received June 20, 2015. Corresponding author: Y. Sato (e-mail: yukisato@em.ist.hokudai.ac.jp).
Digital Object Identifier (inserted by IEEE).

II. Magneto-Quasi-Static Analysis

We consider magneto-quasi-static fields governed by the equations given by

$$\mathrm{rot}\,\nu\mathrm{rot}\boldsymbol{A} + \mathrm{j}\omega\kappa(\boldsymbol{A} + \mathrm{grad}\,\varphi) = 0 \tag{1a}$$

$$\mathrm{div}\{\mathrm{j}\omega\kappa(\boldsymbol{A} + \mathrm{grad}\,\varphi)\} = 0 \tag{1b}$$

are solved, where $\boldsymbol{A}$, φ, ν, ω and κ are vector potential, scalar potential, magnetic reluctivity, angular frequency and conductivity, respectively. Applying the weighted residual method, we can obtain a system of algebraic equations which composes symmetric and sparse FE matrix, that is,

$$\int_\Omega (\mathrm{rot}\boldsymbol{N}_i \cdot \nu\mathrm{rot}\boldsymbol{A} + \mathrm{j}\omega\kappa\boldsymbol{N}_i \cdot \boldsymbol{A})\mathrm{d}V + \int_\Omega \mathrm{j}\omega\kappa\boldsymbol{N}_i \cdot \mathrm{grad}\,\varphi\mathrm{d}V = 0 \tag{2a}$$

$$\int_\Omega \mathrm{j}\omega\kappa\boldsymbol{A} \cdot \mathrm{grad}N_u\mathrm{d}V + \int_\Omega \mathrm{j}\omega\kappa\mathrm{grad}\,\varphi \cdot \mathrm{grad}N_u\mathrm{d}V = 0 \tag{2b}$$

We solve (2) using the ICCG method. From solution of (2), we can calculate the current which flows in the conductor.

$$i = \int_\Omega \mathrm{j}\omega\kappa\boldsymbol{A} \cdot \sum_{\Gamma_{in}\in u}\mathrm{grad}N_u\mathrm{d}V + \int_\Omega \kappa\mathrm{grad}\,\varphi \cdot \sum_{\Gamma_{in}\in u}\mathrm{grad}N_u\mathrm{d}V \tag{3}$$

where Γ_{in} is the input surface of the conductor.

III. Generation of Equivalent Circuit Using PVL

A. Transfer function of linear system

We can rewrite (2) and (3) in the following form

$$\mathrm{N}\dot{\boldsymbol{x}} + \mathrm{K}\boldsymbol{x} = \boldsymbol{b}v_0 \tag{4a}$$

$$i = \boldsymbol{l}^t\boldsymbol{x} \tag{4b}$$

where N, $\mathrm{K}\in\mathrm{R}^{n\times n}$, $\boldsymbol{b}$, $\boldsymbol{l}$, $\boldsymbol{x}=[\boldsymbol{a}, \boldsymbol{\varphi}, i]^t\in\mathrm{R}^n$, respectively, where n denotes degree of freedoms of the FE equation. The unknown

vector $\boldsymbol{x}$ is composed of vector and scalar potentials as well as current. The transfer function of this system can be expressed by

$$\mathrm{H}(s) = \boldsymbol{l}^t(\mathrm{K}+s\mathrm{N})^{-1}\boldsymbol{b} \tag{5}$$

Moreover, H(s) is expressed around the expansion point s_0 as

$$\mathrm{H}(s_0+\sigma) = \boldsymbol{l}^t(\mathrm{I}-\sigma\mathrm{X})^{-1}\boldsymbol{r} \tag{6}$$

where $\mathrm{X}=-(\mathrm{K}+s_0\mathrm{N})^{-1}\mathrm{N}$ and $\boldsymbol{r}=(\mathrm{K}+s_0\mathrm{N})^{-1}\boldsymbol{b}$. We apply spectral decomposition to X in (6) to obtain

$$\mathrm{H}(s_0+\sigma) = \boldsymbol{l}^t(\mathrm{I}-\sigma\mathrm{S}\Lambda\mathrm{S}^{-1})^{-1}\boldsymbol{r} = \sum_{i=1}^{n}\frac{f_i g_i}{1-\sigma\lambda_i} \tag{7}$$

where Λ and S are matrices including the eigenvalues and eigenvectors of X, $\boldsymbol{f}=\mathrm{S}^t\boldsymbol{l}$ and $\boldsymbol{g}=\mathrm{S}^{-1}\boldsymbol{r}$, respectively. It is possible to obtain the equivalent circuit from (7). However, this formulation would be unsuitable for real uses because of heavy computational burden in solution of the eigenvalue problem. To circumvent the above difficulty, we apply the Neumann series expansion to (6)

$$\mathrm{H}(s_0+\sigma) = \boldsymbol{l}^t(\mathrm{I}+\sigma\mathrm{X}+\sigma^2\mathrm{X}^2+\cdots)\boldsymbol{r} = \sum_{i=0}^{\infty} m_i\sigma^i \tag{8}$$

where $m_i = \boldsymbol{l}^t\mathrm{X}^i\boldsymbol{r}$. Effective evaluation of X^i in (8) could be performed by the Lanczos method. However, the Lanczos method is valid for eigenvalue computation of symmetric matrices, while X is generally non-symmetric. For this reason, we employ here the bi-Lanczos method [9] which is valued for non-symmetric matrices. This method seeks for a tridiagonal matrix whose eigenvalues correspond to the significant eigenvalues of the non-symmetric matrix X. The algorithm for bi-Lanczos method is described below.

-----bi-Lanczos method algorithm-------

0) Set $\rho_1=\|\boldsymbol{r}\|_2$, $\eta_1=\|\boldsymbol{l}\|_2$, $\boldsymbol{v}_1=\boldsymbol{r}/\rho_1$, $\boldsymbol{w}_1=\boldsymbol{l}/\eta_1$, $\boldsymbol{v}_0=\boldsymbol{w}_0=0$ and $\delta_0=0$

For n=1,2…,q do

1) Compute $\delta_n=\boldsymbol{w}_n^t\boldsymbol{v}_n$
2) Set $\alpha_n=\boldsymbol{w}_n^t\mathrm{X}\boldsymbol{v}_n/\delta_n$, $\beta_n=\eta_n\delta_n/\delta_{n-1}$, $\gamma_n=\rho_n\delta_n/\delta_{n-1}$
3) Set $\boldsymbol{v}=\mathrm{X}\boldsymbol{v}_n-\alpha_n\boldsymbol{v}_n-\beta_n\boldsymbol{v}_{n-1}$, $\boldsymbol{w}=\mathrm{X}^t\boldsymbol{w}_n-\alpha_n\boldsymbol{w}_n-\gamma_n\boldsymbol{v}_{n-1}$
4) Set $\rho_{n+1}=\|\boldsymbol{v}\|_2$, $\eta_{n+1}=\|\boldsymbol{w}\|_2$
   $\boldsymbol{v}_{n+1}=\boldsymbol{v}/\rho_{n+1}$, $\boldsymbol{w}_{n+1}=\boldsymbol{w}/\eta_{n+1}$

In this algorithm, we have to solve the FE equation twice to calculate $\mathrm{X}\boldsymbol{v}_n$ and $\mathrm{X}^t\boldsymbol{w}_n$. Applying the bi-Lanczos method to X, we obtain the two tridiagonal matrices of the form

$$\mathrm{T}_q = \begin{bmatrix} \alpha_1 & \beta_2 & 0 & \cdots & 0 \\ \rho_2 & \alpha_2 & \beta_3 & \ddots & \vdots \\ 0 & \rho_3 & \ddots & \ddots & 0 \\ \vdots & \ddots & \ddots & \ddots & \beta_q \\ 0 & \cdots & 0 & \rho_q & \alpha_q \end{bmatrix}, \tilde{\mathrm{T}}_q = \begin{bmatrix} \alpha_1 & \gamma_2 & 0 & \cdots & 0 \\ \eta_2 & \alpha_2 & \gamma_3 & \ddots & \vdots \\ 0 & \eta_3 & \ddots & \ddots & 0 \\ \vdots & \ddots & \ddots & \ddots & \gamma_q \\ 0 & \cdots & 0 & \eta_q & \alpha_q \end{bmatrix} \tag{9}$$

where

$$\mathrm{X}\mathrm{V}_q = \mathrm{V}_q\mathrm{T}_q, \quad \mathrm{X}^t\mathrm{W}_q = \mathrm{V}_q\tilde{\mathrm{T}}_q \tag{10}$$

In (10), V_q and W_q represent the matrices whose columns are $\boldsymbol{v}_n$ and $\boldsymbol{w}_n$. The following relation is given by

$$\tilde{\mathrm{T}}_q = \mathrm{D}_q\mathrm{T}_q\mathrm{D}_q^{-1}, \quad \mathrm{D}_q = \mathrm{diag}\begin{bmatrix}\delta_1 & \cdots & \delta_n\end{bmatrix} \tag{11}$$

B. *Padé approximation via the Lanczos process* [3]

First, we evaluate m_i in (8) using the bi-Lanczos method as follows:

$$m_i = \boldsymbol{l}^t\mathrm{X}^i\boldsymbol{r} = \boldsymbol{l}^t\boldsymbol{r}(\boldsymbol{e}_1^t\mathrm{T}_q^i\boldsymbol{e}_1) \tag{12}$$

where $\boldsymbol{e}_1=[1,0,\ldots,0]^t$. Substituting (12) into (8), we obtain

$$\mathrm{H}(s_0+\sigma) = \sum_{i=0}^{\infty}\boldsymbol{l}^t\boldsymbol{r}(\boldsymbol{e}_1^t\mathrm{T}_q^i\boldsymbol{e}_1)\sigma^i = \boldsymbol{l}^t\boldsymbol{r}\boldsymbol{e}_1^t(\mathrm{I}-\sigma\mathrm{T}_q)^{-1}\boldsymbol{e}_1 \tag{13}$$

Next, we perform the spectrum decomposition for T_q to obtain

$$\begin{aligned}\mathrm{H}(s_0+\sigma) &= \boldsymbol{l}^t\boldsymbol{r}\boldsymbol{e}_1^t(\mathrm{I}-\sigma\mathrm{S}_q\Lambda_q\mathrm{S}_q^{-1})^{-1}\boldsymbol{e}_1 \\ &= \sum_{j=1}^{q}\frac{\boldsymbol{l}^t\boldsymbol{r}\mu_j\nu_j}{1-\sigma\lambda_j}\end{aligned} \tag{14}$$

where $\boldsymbol{\mu}=\mathrm{S}_q^t\boldsymbol{e}_1$ and $\boldsymbol{\nu}=\mathrm{S}_q^{-1}\boldsymbol{e}_1$. Note that the size of T_q is much smaller than that of X. Hence we can effectively perform the spectrum decomposition of T_q. Finally, we obtain the reduced transfer function

$$\mathrm{H}(s_0+\sigma) = k_\infty + \sum_{\substack{j=1\\ \lambda_j\neq 0}}^{q}\frac{k_j}{\sigma-p_j} \tag{15}$$

where

$$k_j = \frac{-\boldsymbol{l}^t\boldsymbol{r}\mu_j\nu_j}{\lambda_j}, \quad k_\infty = \sum_{\substack{j=1\\ \lambda_j=0}}^{q}\boldsymbol{l}^t\boldsymbol{r}\mu_j\nu_j, \quad p_j = \frac{1}{\lambda_j} \tag{16}$$

which corresponds to the Padé approximation of the transfer function (6). In this processes, we can also employ Block-Arnoldi Algorithm [10] to construct (15) from (5).

C. *Generation of equivalent circuit*

The reduced transfer function (15) can be regarded as an admittance function $\mathrm{Y}(s_0+\sigma)$ because the input and output of (4) are voltage and current, respectively. The expansion point is set to $s_0=2\pi f_{\max}$.

Here, the admittance function (15) is expressed by

$$Y(s_0+\sigma)=\frac{1}{Z_\infty}+\frac{1}{Z_1}+\frac{1}{Z_2}+\cdots+\frac{1}{Z_q} \tag{17}$$

Substituting $\sigma=s-s_0=\mathrm{j}\omega-2\pi f_{\max}$ to (15), we have

$$Z_j=\frac{-2\pi f_{\max}-p_j}{k_j}+\mathrm{j}\omega\frac{1}{k_j}=R_j+\mathrm{j}\omega L_j \tag{18}$$

where R_j and L_j obtained by this method are resistance and inductance for the Foster equivalent circuit shown in Fig. 1. Note that $|p_j|>2\pi f_{\max}$ must hold so that the condition $R_j\geq 0$ is satisfied.

IV. Numerical Results

A. Coil windings model

We apply the proposed method to the coil windings model shown in Fig. 2 in which κ is set to 5.76×10^7S/m. The scalar potential are defined on the cross-sectional surface of the coil as follows [11] :

$$\varphi=\varphi_0\sum_{\Gamma_{in}\in n}N_n+\sum_j\varphi_j\sum_{\Gamma_j\in n}N_n \tag{19}$$

where Γ_{in} and Γ_j denote the input and other cross-sectional surfaces of the coil windings. Because the coil windings are connected in series, the identical scalar potentials are assumed on the common surfaces.

The frequency range of interest is $0\leq f\leq 1$MHz. Due to symmetry, we analyze one eighth of the coil windings model. We employed 298201 tetrahedral elements in the FE model.

The frequency characteristics for the impedance are shown in Fig. 3 in which "FEM" and "$q=i$" indicate the results obtained by conventional FE analysis and the resultant equivalent circuit, in which i is number of stages of the Foster circuit. We conclude from Fig. 3 that the equivalent circuit is rather accurate even if q=2. We summarize the values of circuit parameters of the Foster circuit in TABLE I.

The computational time for generation of the Foster circuit is about 40 min when q=5 using Xeon W5590/3.2GHz(12GB RAM). On the other hand, the elapsed time of field computations by FEM at 13 sampling frequencies shown in Fig. 3 is 230 min under the same computational environment. This method would be very effective for design of external circuit connected to electromagnetic machines and devices because of its light computational burden and accuracy.

B. Inductor model for DC-DC converter

An inductor included in a simple DC-DC converter shown in Fig. 4 is analyzed by FEM. The core material of the inductor is magnetically saturated under DC bias condition. Moreover, the skin and proximity effects in the coil windings become significant when the switching frequency increases. Although the FE equation of the inductor can be simultaneously solved with the circuit equation, this coupling analysis would take too long time for circuit design. The equivalent circuit model of the inductor, which is accurate in a wide frequency range, is not only effective for design of this circuit, but also for other circuits.

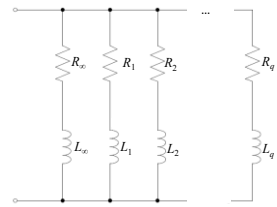

Fig. 1 Foster Circuit

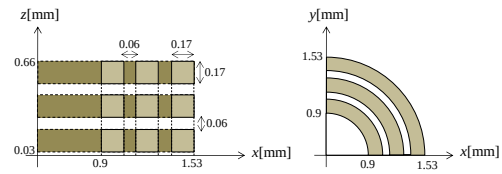

Fig. 2 Coil windings model (axial symmetry).

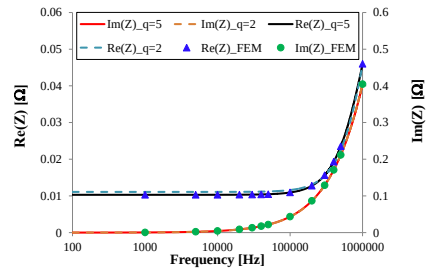

Fig. 3 Frequency characteristic of Impedance for coil windings.

TABLE I

Circuit parameters obtained by present method.

q	R_1[Ω]	R_2[Ω]	R_3[Ω]	R_4[Ω]	R_5[Ω]
5	1.03e-2	5.69	6.82	141	58.3
2	1.11e-2	3.51	----	----	----
q	L_1[H]	L_2[H]	L_3[H]	L_4[H]	L_5[H]
5	6.97e-8	8.02e-7	7.25e-7	1.31e-6	1.79e-6
2	6.89e-8	3.18e-7	----	----	----

The biased DC current flowing through the inductor windings used in DC-DC converters is superimposed with an AC current of small amplitude. To determine the operation point, we analyze the magneto-static field considering magnetic saturation by solving

$$\mathrm{rot}\,\nu(\boldsymbol{A})\mathrm{rot}\boldsymbol{A}=\boldsymbol{j}i_{bs} \tag{20}$$

where $\boldsymbol{j}$ and i_{bs} are the current density whose integration over a cross-section results in unit current, and the magnitude of the biased DC current. From this analysis, we can determine the different values of permeability in the FEs. Then assuming that the permeability values are frozen to these ones, we solve linear Maxwell equations to create the equivalent circuit using the method mentioned in Section III. This method is expected to be accurate in the steady state, while it might be inaccurate in the transient states where permeability is significantly different from that in the steady state.

Fig. 5 shows the inductor model used in the DC-DC converter shown in Fig. 4 where the core material and the conductivity of the coil winding are assumed to be 50A400 and 5.76×10^7S/m. The pulse frequency, the duty factor, resistance R_0 and capacitance C_0 in Fig. 5 are set to 1MHz, 0.9, 0.05Ω and 1μF, respectively. Moreover, the number of the

stages for the Foster circuit is set to 5 and DC voltage is assumed to be either 0.3V or 1.2V. The corresponding biased currents are 5A and 20A. We discretize the FE domain of the inductor model with 117548 tetrahedral elements.

The currents flowing through L_{FEM} are shown in Figs. 6 and 7 where "static" represents the result which is obtained from a circuit model in which the inductor is modeled as pure inductance neglecting eddy current losses. Moreover, "present" and "FEM" represent the results which are obtained from the equivalent circuit constructed by the proposed method and coupled FE-circuit analysis, respectively. It is found from Fig. 6 that the current obtained by present method agrees well with that obtained by the coupled FE-circuit analysis. We can find some differences in them in Fig. 7. The reason of these differences is that the dynamic changes in the permeability become significant when E is increased to 1.2V, and thus the assumption of the frozen permeability gives rise to errors. The computational time for circuit generation of the inductor is about 13 min. under the same computational environment mentioned above. The coupled FE-circuit analysis considering nonlinearity of the inductor core, skin and proximity effects takes more than 6 hours. Note that the elapsed time of the circuit analysis is negligibly shorter than the coupled FE-circuit analysis. Once we construct the equivalent circuit, the circuit analysis can be effectively performed changing the topology and parameters for circuit design.

V. Conclusion

In this paper, we have proposed a novel method to generate equivalent circuits using MOR based on PVL. This method has been applied to the coil windings model and inductor model used in a DC-DC converter. The proposed method can take the eddy current effects and nonlinearity of core materials into account. The equivalent circuit constructed by the proposed method is accurate when the nonlinearity is not strong and the computational time is much shorter than that of FE-circuit coupling analysis. In this work we neglect capacitance between the coils which becomes significant in higher frequency range. In future work, we plan to include the capacitive effects in the equivalent circuit.

Acknowledgment

This work was supported in part by JSPS KAKENHI Grant Number 25630101 and 15J01550 as well as JSPS and CAPES under the Japan-Brazil Research Cooperative Program.

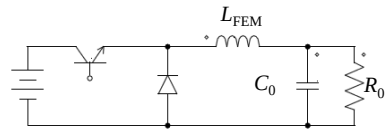

Fig. 4 DC-DC converter

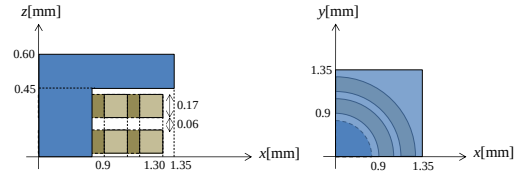

Fig. 5 Inductor model.

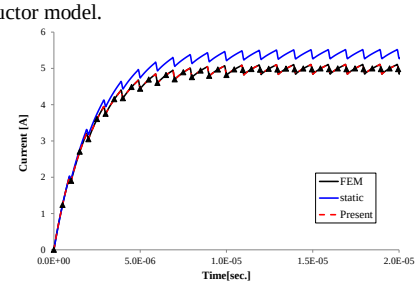

Fig. 6 Current obtained by present method and FEM when E=0.3V.

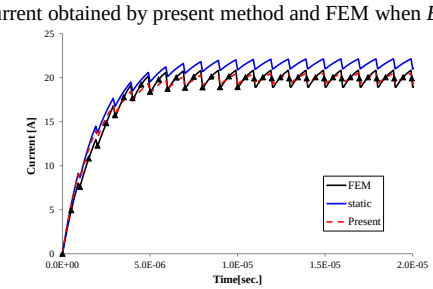

Fig. 7 Current obtained by present method and FEM when E=1.2V.

TABLE II
Circuit parameters obtained by present method.

i_{bs}	R_1[Ω]	R_2[Ω]	R_3[Ω]	R_4[Ω]	R_5[Ω]
5A	4.13e-2	10.3	985	327	804
20A	4.13e-2	11.4	969	322	683
i_{bs}	L_1[H]	L_2[H]	L_3[H]	L_4[H]	L_5[H]
5A	1.11e-7	1.59e-6	8.71e-6	9.55e-6	5.70e-6
20A	9.55e-8	1.77e-6	8.68e-6	9.80e-6	4.79e-5

Reference

[1] B. Gustavsen, A. Semlyen, "Rational Approximation of Frequency Domain Responses by Vector Fitting," *IEEE Trans. Power Delivery*, vol. 14, no. 3, pp. 1052-1061, 1999.

[2] Y. Shindo, O. Noro, "Simple Circuit Simulation Models for Eddy Current in Magnetic Sheets and Wires," *IEEJ Trans. Fundamentals and Materials*, vol. 134, no. 4, pp. 173-181, 2014.

[3] P. Feldmann and R. A. Freund, "Efficient Linear Circuit Analysis by Padé Approximation via the Lanczos Process," *IEEE Trans. Computer-Aided Design*, vol. 14, no. 5, pp. 639–649, May 1995.

[4] M. Celik, A. C. Cangellaris, "Simulation of Dispersive Multiconductor Transmission Lines by Padé Approximation via the Lanczos Process," *IEEE Trans. Microwave Theory and Techniques*, vol. 1996.

[5] D. Schmidthäusler S. Schöps and M. Clemens, "Reduction of Linear Subdomain for Non-Linear Electro-Quasistatic Field Simulation," *IEEE Trans. Magn.*, vol. 49, no. 5, pp, 1669-1672, May. 2013.

[6] Y. Sato and H. Igarashi, "Model Reduction Based on the Method of Snapshots for Eddy Current Problems," *IEEE Trans. Magn*, vol. 49, no. 5, pp. 1697-1700, May, 2013.

[7] T. Henneron and S. Clénet, "Model Order Reduction of Nonlinear Magnetostatic Problems Based on POD and DEI Methods," *IEEE Trans. Magn*, vol. 50, no. 2, Feb., 2014.

[8] T. Shimotani, Y. Sato and H.Igarashi, "Generation of Equivalent Circuit from Finite Element Model of Electromagnetic Devices Using Proper Orthogonal Decomposition," *Abstract of Compumag2015*, .

[9] C. Lanczos, "An iteration method for the solution of the eigenvalue problem of linear differential and integral operators," *J. Res. Nat. Bur. Standards*, vol. 45, pp. 255-282, 1950.

[10] D. L. Boley, "Krylov Space Methods on State-Space Control Models", *Circuits Syst. Signal Process*. vol.13, no.6, pp. 733-758, 1994

[11] P. Dular, F. Henrotte and W. Legros, "A General and Natural Method to Define Circuit Relations Associated with Magnetic Vector Potential Formulations," *IEEE Trans. Magn*, vol. 35, no. 3, pp. 1630-1633, May, 1999.